

Article

Deterministic Methodology for Determining the Optimal Sampling Frequency of Water Quality Monitoring Systems

Mahmoud S. Al- Khafaji*

Civil Engineering Department, University of Technology - Iraq; 41100@uotechnology.edu.iq

* Correspondence: 41100@uotechnology.edu.iq; +9647801618485

Abstract: This paper proposes a novel deterministic methodology for estimating the optimal sampling frequency (SF) of water quality monitoring systems. The proposed methodology is based on employing two-dimensional contaminant transport simulation models to determine the minimum SF considering all the potential changes in the boundary conditions of a water body. A two-dimensional contaminant transport simulation model (RMA4) was implemented to estimate the distribution patterns of the total dissolved solids (TDS) within the Al-Hammar Marsh in the southern part of Iraq for 30 cases of potential boundary conditions. Using geographical information system (GIS) tools, a spatiotemporal analysis approach was applied to the results of the RMA4 model to determine the minimum SF of the monitoring stations with an accuracy level of detectable change in TDS concentration (ALC) of 5%, 10% and 15%. The proposed methodology specified a minimum and maximum SF for each monitoring station (MS) that ranged between 12 and 33 times per year, respectively. Additionally, increasing the ALC to 10% and 15% increase the minimum SF for some MSs by approximately 18% and 21%, respectively. However, the proposed methodology includes all the potential values and cases of boundary conditions, which increases the certainty of monitoring the system and the efficiency of the SF schedule. Moreover, the proposed methodology can be effectively applied to all types of surface water resources.

Keywords: Sampling frequency; deterministic approach; simulation model; water quality.

1. Introduction

Water pollution is a growing menace to natural ecosystems and human life. The distribution of pollution within a water resource system is characterized by significant spatial and temporal variations due to differences in hydrological conditions and pollution sources. Overcoming this challenge requires better understanding of the spatial and temporal variations in the distribution of pollutants within aquatic systems [1]. An efficient assessment of the water quality (WQ) within a water resource system is highly dependent on the efficiency of the monitoring network (MN). However, obtaining the optimal design of water quality monitoring networks (WQMN) is a very complex process due to the large number of factors that must be considered, such as monitoring objectives, water quality parameters, monitoring station locations and sampling frequency (SF) [2]. Accordingly, SF is a very important variable in the design of WQMN. An appropriate SF ensures that no pollution surge passes a monitoring station (MS) without being detected. The design aspects of WQMN have been widely considered since the 1940s [2]. Additionally, the optimal design of a WQMN considering the SF and all issues related to the improvement of monitoring program efficiency have been widely addressed in the literature [3, 4]. After the 1980s, many attempts were carried out to improve monitoring efficiency with regard to the problem constraints and design criteria [5-7]. Subsequently, the optimal design of WQMN was discussed in [8], and the basic principles of WQMN design and criteria of allocating WQMSs were applied in [9-12]. Thereafter, many studies in the 1990s covered topics concerned with specifying the SF, such as [13-18]. Moreover, integer programming and multiobjective programming in which more complex issues

were addressed were used to assess the SF [19-21]. A comprehensive review of these papers can be found in [22]. [23] presented sampling frequencies for the Global Environment Monitoring System for freshwater (GEMS/Water) baseline and trend stations, as shown in Table 1.

Table 1. Sampling frequency for GEMS/WATER stations [23].

Water body		Sampling frequency
Baseline stations	Streams	Minimum: 4 per year, including high- and low-water stages. Optimum: 24 per year (every second week); weekly for total suspended solids.
	Headwater lakes	Minimum: 1 per year at turnover; sampling at lake outlet. Optimum: 1 per year at turnover, and 1 vertical profile at the end of stratification season.
	Rivers	Minimum: 12 per year for large drainage areas (approximately 100,000 km ²). Maximum: 24 per year for small drainage areas (approximately 10,000 km ²).
Trend stations	Lakes and reservoirs	For issues other than eutrophication: Minimum: 1 per year at turnover. Maximum: 2 per year at turnover, and 1 at maximum thermal stratification. For eutrophication: 12 per year, including twice monthly during the summer.
	Groundwater	Minimum: 1 per year for large, stable aquifers. Maximum: 4 per year for small, alluvial aquifers. Karst aquifers: same as rivers.

The effective design of a WQMN was considered using various types of statistical and/or programming techniques, such as integer programming, multiobjective programming, kriging theory and optimization analysis [19-21, 14, 24, 25]. Additionally, statistical approaches used for the assessment and redesign of WQMN were reviewed by [26]. In this review, various monitoring objectives and related assessment and redesign methods of long-term WQMN were discussed. Based on the pollution level to be detected and variability of the WQ data, a statistical approach is commonly used to estimate the WQ SF [27]. The statistical tools that are commonly used to optimize the temporal frequency of monitoring in WQ networks are confidence intervals, trend analyses, geostatistical tools, multivariate analyses, optimization programs, entropy analyses and artificial neural networks [26]. Two quantitative measures of the effectiveness of different sampling frequencies were proposed by [28]. These measures are destined to be utilized at the preliminary design stage to detect violations of WQ standards. The analytic hierarchy process (AHP), which is an effective method for decision analysis, was applied to analyze environmental impact assessments [29] and design river WQ SF [30].

In recent years, computer-aided mathematical simulation models of water quality have been rapidly developed [31]. Such models can be used to predict water quality by accounting for changes that affect water quality factors or changes in their intensity. Two-dimensional models (2D) are used most often in the case of lakes, reservoirs or deep rivers. The end result of these models is an estimation of water quality parameters close to measurements of actual concentrations. Assessment of individual parameters can be performed for given time intervals: hourly, daily, weekly, monthly and yearly [32]. Integral utilization of simulation models and the tools and facilities of geographical

information systems (GIS) can assist and support developing new efficient approaches to obtain the optimal design of a WQMN.

However, a comprehensive review of the abovementioned literature showed that WQMNs have traditionally been designed on the basis of a measured dataset collected from nonoptimal preallocated monitoring stations (MSs). Additionally, an assessment of the monitoring efficiency of the stations of a WQMN was implemented using statistical methods and general criteria. These methods and criteria are applied to insufficient datasets because some effective events or values, which are required for achieving the monitoring objectives, may not be detected because of the inadequacy of the locations and SFs of the MSs. Consequently, the obtained level of monitoring accuracy is based on the number of detected events according to these MSs, which does not account for all the events that have occurred or the potential of future events. Moreover, the effects of changes in boundary conditions, land cover and land use on optimal SF are not taken into consideration. The update, reanalysis, reassessment and reuse of a WQMN database using the traditional method are very difficult.

This paper aims to present a new deterministic approach for employing the features and facilities of the hydrodynamic simulation models of contaminant transport to specify the optimal SF for each MS in the WQMN according to all potential changes in the boundary conditions of a water body. Furthermore, maximizing the monitoring accuracy of each MS and subsequently the overall WQMN decreases the cost, time and effort of monitoring. The optimal allocation of the MS was not considered as an aim of this study. This paper concerns specifying the SF schedule for prespecified optimal locations of MSs in a WQMN.

2. Materials and Methods

2.1. Methodology

The computation of SF is based on specifying the minimum interval between successive detectable changes in the value or concentration of a WQ parameter at an MS. However, the SF must be sufficient to detect the change in WQ within an accuracy level specified according to the monitoring objectives. This SF must ensure detection of the entire pollution surges that passes an MS. This MS should be located at the optimal position where it is most sensitive to changes in the WQ.

The WQ distribution patterns and the velocity and time of contaminant transport can be estimated by using hydrodynamic and contaminant transport simulation models. Two-dimensional simulation models are sufficient tools for studying the transport of contaminants within lakes, reservoirs, or deep rivers [32].

The time scale of the SF is usually greater than one day. Additionally, the differences in the diffusion velocities of contaminants caused by the variations in the diffusion and dispersion coefficients in some bodies of water, such as the considered marsh, are not large enough to make a difference in transport time of the contaminants between the MSs greater than one day. Therefore, the total dissolved solids (TDS) can be considered the representative parameter instead of other water quality parameters. Moreover, unlike other water quality parameters, sufficient records of TDS data are available. Accordingly, the required level of TDS monitoring accuracy (the detectable change in TDS concentration) (ALC) can be adopted as the required level of monitoring accuracy at the MSs. The recommended accuracy (uncertainty levels) expressed at the 95% confidence interval is $\pm 5\%$ [33]. Consequently, the minimum interval of SF in an MS should be the minimum time interval between two successive $\pm 5\%$ changes in TDS concentration.

When there is a large number of spatially relevant data, the spatial analysis tools of geographical information systems (GIS) can be utilized to address such data. Therefore, these tools can be employed to determine the SF of all the WQ MSs within the study area.

The methodology of the proposed approach can be summarized as follows:

- i. Specify the study area and collect the topography data of the study area, locations of the preallocated MSs of the considered WQMN and recorded discharge, water depth and WQ datasets at the inlet, outlet and within the water body.
- ii. Analyze the hydraulic and WQ datasets, which is the TDS data in this study, to specify all the potential cases and values of the boundary conditions for the study area. Consequently, the required calibration and verification datasets should be specified according to these cases.
- iii. Implement the hydrodynamic and contaminant transport simulation models. Before applying these models for all potential cases of boundary conditions, the calibration and verification processes should be performed.
- iv. Based on the results of the contaminant transport simulation model, utilize the spatiotemporal analysis tools of GIS to obtain the temporal changes in the TDS distribution patterns within the marsh. Subsequently, compute the minimum time interval of detecting a successive change in the concentration of TDS at each MS with an ALC of $\pm 5\%$ for each case of boundary conditions.
- v. To evaluate the effect of changing the ALC, reanalyze the results of the contaminant transport simulation model (TDS distribution patterns) using the spatiotemporal analysis approach and increasing ALC to $\pm 10\%$ and $\pm 15\%$ for each case of boundary conditions.
- vi. To verify the proposed methodology, a sampling schedule can be implemented based on the criteria of the sampling frequency for GEMS/WATER stations [23] to compare with the results produced by using the proposed methodology.
- vii. Analyze and discuss the results and present the main conclusions and recommendations.

2.2. Study Area

The western part of the Al-Hammar Marsh is located within the southeastern part of the Thi-Qar Governorate in southern Iraq (Figure 1). The Al-Hammar Marsh has an area of approximately 1350 km^2 and a maximum water depth of 1.8 m a.s.l. The marsh has a complex feeding and outlet system. Some of the marsh feeders, which are denoted BC3, BC4, FBC3, FBC4 and FW, are short channels that convey the water directly from the Euphrates River to the marsh. These feeders work as feeders and/or outlets according to the levels of the water surface in the marsh and Euphrates River. In contrast, other feeders, such as Um Nakhla, Al-Kurmashia, Al-Qausy Drain and Al-Hamedy, convey the water from a reach of the Euphrates River upstream of the marsh to the western zone of the marsh. Additionally, some of the main outfall drain (MOD) water is discharged into the marsh through the Al-Khamissiya Canal. The main outlet of the marsh is the Al-Hammar Outlet, which is located downstream of the eastern zone of the marsh.

The marsh boundary and locations of the most sensitive WQ MSs for this part of the Al-Hammar Marsh were specified by [34], as shown in Figure 2.

A digital elevation model (DEM) for the study area, shown in Figure 3, was created by using the topographical survey data provided by the General Directorate of Survey/MoWR in May 2017 (unpublished data).

[35] obtained and verified the roughness-depth relationship of the marsh bed given by Manning's roughness coefficients, as shown in Figure 4. The annual average evapotranspiration (ET_o) of the marsh is 2909.3 mm according to the [36].

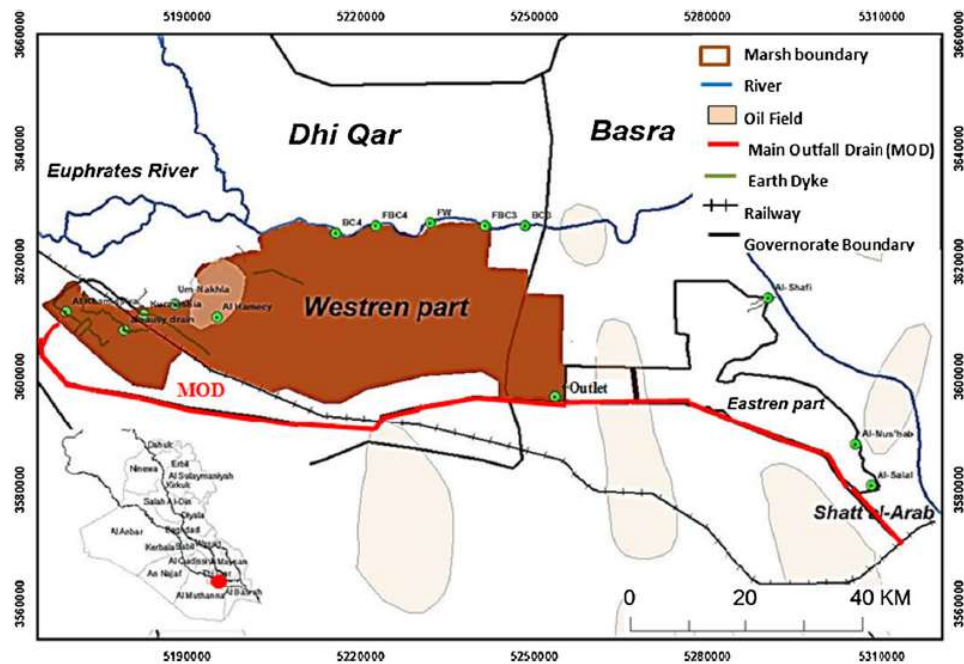


Figure 1. Layout of the Al-Hammar Marsh [34].

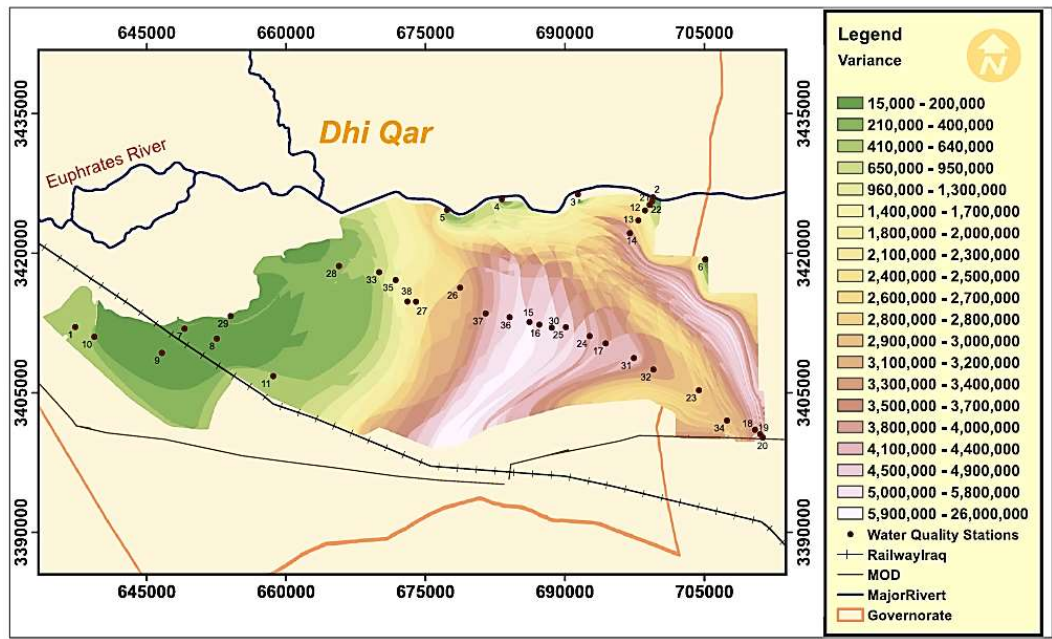


Figure 2. Locations of the most sensitive WQ MSs for the western part of the Al-Hammar Marsh [34].

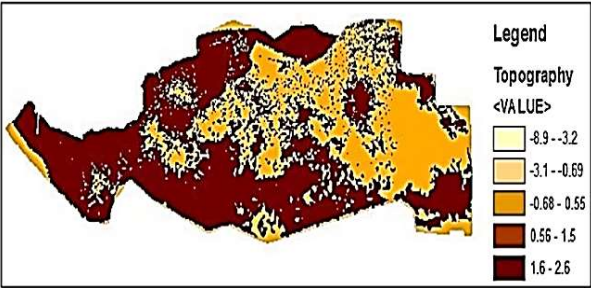


Figure 3. Topography of the Al-Hammar Marsh.

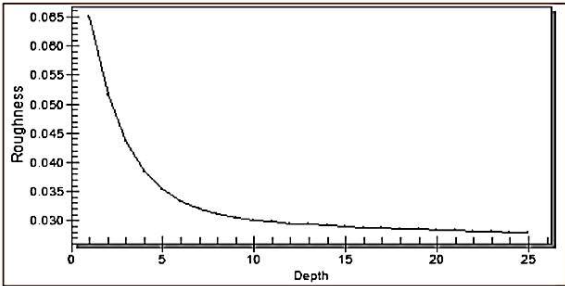


Figure 4. Manning's roughness coefficients of the Al-Hammar Marsh [35].

The Center for the Restoration of Iraqi Marsh and Wetland (CRIMW) provided the recorded discharge, water surface elevation and concentration of TDS at the inlet, outlet and within the marsh for the period of 2010 to 2017 (unpublished data). These datasets were analyzed to specify the potential cases and values of the marsh boundary conditions for the water quantity and quality aspects. According to the requirements of the hydrodynamic and contaminant transport simulation models, these boundary conditions can be represented by 30 cases (see Tables 2 and 3).

Field investigation measurements were carried out to prepare the required datasets for performing the verification process of the simulation models. The period of carrying out these measurements was from 3 May 2015 to 28 May 2015. These measurements included the flow velocity, water depth and TDS concentration at 31 positions within the marsh area in addition to the discharge and concentration of TDS at the inlets and outlets of the marsh, whereas the water surface elevation (WSE) was measured at the outlet of the marsh. Figure 5 shows the locations of the measurement positions. The results of these measurements are listed in Tables 4 and 5.

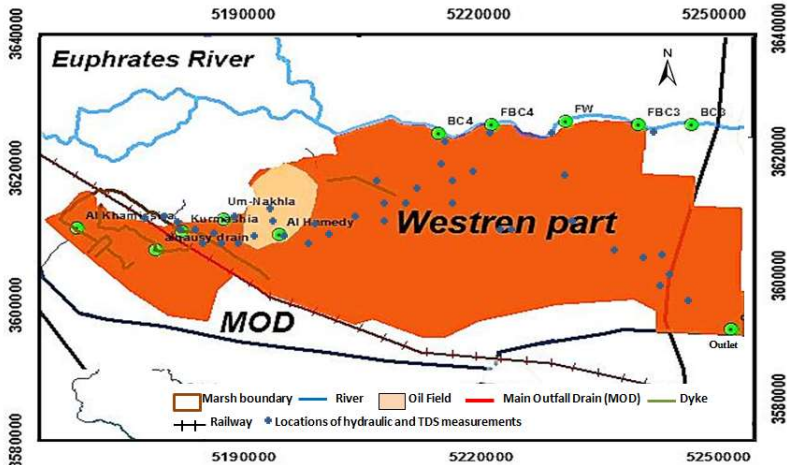


Figure 5. Locations of the measurement positions.

Table 2. Potential cases of marsh boundary conditions for the hydrodynamic simulation model (CRIMW 2017 (unpublished data)).

Case No.	Discharge (m3/sec)										WSE (m a.s.l.)
	BC3	BC4	FBC3	FBC4	FW	Um Nakhla	Al-Kurmashia	Al-Qausy Drain	Al-Hamedy	Al-Khamissiya	Hammar Outlet
1	3.93	3.83	4.60	5.50	10.00	6.85	3.85	29.63	5.30	56.55	1.90
2	3.93	3.83	4.60	5.50	10.00	6.85	3.85	29.63	5.30	26.38	1.90
3	3.93	3.83	4.60	5.50	10.00	6.85	3.85	29.63	5.30	9.70	1.90
4	1.82	2.19	1.87	1.95	2.08	3.14	1.76	13.25	1.97	56.55	1.90
5	1.82	2.19	1.87	1.95	2.08	3.14	1.76	13.25	1.97	26.38	1.90
6	1.82	2.19	1.87	1.95	2.08	3.14	1.76	13.25	1.97	9.70	1.90
7	0.43	0.50	0.50	0.45	0.35	0.85	0.35	3.00	0.20	56.55	1.90
8	0.43	0.50	0.50	0.45	0.35	0.85	0.35	3.00	0.20	26.38	1.90
9	0.43	0.50	0.50	0.45	0.35	0.85	0.35	3.00	0.20	9.70	1.90
10	3.93	3.83	4.60	5.50	10.00	6.85	3.85	29.63	5.30	56.55	1.67
11	3.93	3.83	4.60	5.50	10.00	6.85	3.85	29.63	5.30	26.38	1.67
12	3.93	3.83	4.60	5.50	10.00	6.85	3.85	29.63	5.30	9.70	1.67
13	1.82	2.19	1.87	1.95	2.08	3.14	1.76	13.25	1.97	56.55	1.67
14	1.82	2.19	1.87	1.95	2.08	3.14	1.76	13.25	1.97	26.38	1.67
15	1.82	2.19	1.87	1.95	2.08	3.14	1.76	13.25	1.97	9.70	1.67
16	0.43	0.50	0.50	0.45	0.35	0.85	0.35	3.00	0.20	56.55	1.67
17	0.43	0.50	0.50	0.45	0.35	0.85	0.35	3.00	0.20	26.38	1.67
18	0.43	0.50	0.50	0.45	0.35	0.85	0.35	3.00	0.20	9.70	1.67
19	3.93	3.83	4.60	5.50	10.00	6.85	3.85	29.63	5.30	56.55	1.35
20	3.93	3.83	4.60	5.50	10.00	6.85	3.85	29.63	5.30	26.38	1.35
21	3.93	3.83	4.60	5.50	10.00	6.85	3.85	29.63	5.30	9.70	1.35
22	1.82	2.19	1.87	1.95	2.08	3.14	1.76	13.25	1.97	56.55	1.35
23	1.82	2.19	1.87	1.95	2.08	3.14	1.76	13.25	1.97	26.38	1.35
24	1.82	2.19	1.87	1.95	2.08	3.14	1.76	13.25	1.97	9.70	1.35
25	0.43	0.50	0.50	0.45	0.35	0.85	0.35	3.00	0.20	56.55	1.35
26	0.43	0.50	0.50	0.45	0.35	0.85	0.35	3.00	0.20	26.38	1.35
27	0.43	0.50	0.50	0.45	0.35	0.85	0.35	3.00	0.20	9.70	1.35
28	3.93	3.83	4.60	5.50	10.00	6.85	3.85	29.63	5.30	0.00	1.90
29	1.82	2.19	1.87	1.95	2.08	3.14	1.76	13.25	1.97	0.00	1.67
30	0.43	0.50	0.50	0.45	0.35	0.85	0.35	3.00	0.20	0.00	1.35

Table 3. Potential cases of marsh boundary conditions for the contaminant transport simulation model (CRIMW 2017 (unpublished data)).

Case No.	TDS (ppm)									
	BC3	BC4	FBC3	FBC4	FW	Um Nakhla	Al-Kurmashia	Al-Qausy Drain	Al-Hamedy	Al-Khamissiya
1	2130	2979	1790	1790	1790	1622	1618	3575	3319	3050
2	2130	2979	1790	1790	1790	1622	1618	3575	3319	4776
3	2130	2979	1790	1790	1790	1622	1618	3575	3319	7012
4	3299	4749	2879	2879	2879	2879	2879	5310	5624	3050
5	3299	4749	2879	2879	2879	2879	2879	5310	5624	4776
6	3299	4749	2879	2879	2879	2879	2879	5310	5624	7012
7	5155	8232	6750	6750	6750	6750	6750	8791	9102	3050
8	5155	8232	6750	6750	6750	6750	6750	8791	9102	4776
9	5155	8232	6750	6750	6750	6750	6750	8791	9102	7012
10	2130	2979	1790	1790	1790	1622	1618	3575	3319	3050
11	2130	2979	1790	1790	1790	1622	1618	3575	3319	4776
12	2130	2979	1790	1790	1790	1622	1618	3575	3319	7012
13	3299	4749	2879	2879	2879	2879	2879	5310	5624	3050
14	3299	4749	2879	2879	2879	2879	2879	5310	5624	4776
15	3299	4749	2879	2879	2879	2879	2879	5310	5624	7012
16	5155	8232	6750	6750	6750	6750	6750	8791	9102	3050
17	5155	8232	6750	6750	6750	6750	6750	8791	9102	4776
18	5155	8232	6750	6750	6750	6750	6750	8791	9102	7012
19	2130	2979	1790	1790	1790	1622	1618	3575	3319	3050
20	2130	2979	1790	1790	1790	1622	1618	3575	3319	4776
21	2130	2979	1790	1790	1790	1622	1618	3575	3319	7012
22	3299	4749	2879	2879	2879	2879	2879	5310	5624	3050
23	3299	4749	2879	2879	2879	2879	2879	5310	5624	4776
24	3299	4749	2879	2879	2879	2879	2879	5310	5624	7012
25	5155	8232	6750	6750	6750	6750	6750	8791	9102	3050
26	5155	8232	6750	6750	6750	6750	6750	8791	9102	4776
27	5155	8232	6750	6750	6750	6750	6750	8791	9102	7012
28	2130	2979	1790	1790	1790	1622	1618	3575	3319	3050
29	3299	4749	2879	2879	2879	2879	2879	5310	5624	3050
30	5155	8232	6750	6750	6750	6750	6750	8791	9102	7012

Table 4. Flow velocity, water depth and TDS within the marsh (measured on 27 May 2015 and 28 May 2015).

Point No.	Location		Flow velocity (m/sec)	Depth (m)	TDS (ppm)
	E	N			
1	735739	3413844	0.014	1.25	3603
2	640266	3411446	0.031	1.25	3280
3	640674	3412158	0.016	1.11	4046
4	641115	3412073	0.027	1.40	4041
5	642122	3411965	0.021	1.31	4041
6	641479	3411141	0.017	0.75	3355
7	649680	3410178	0.031	0.90	3525
8	653389	3410968	0.024	0.75	1930
9	657249	3410967	0.016	1.56	3543
10	657072	3410796	0.008	2.80	3669
11	656077	3410371	0.012	0.97	2802
12	655028	3410202	0.028	0.93	3495
13	654336	3409881	0.036	0.74	3700
14	653581	3409873	0.031	1.84	3575
15	653351	3409814	0.032	0.95	3609
16	652953	3410096	0.029	1.24	3635
17	652563	3409957	0.035	1.70	3640
18	652055	3409220	0.031	1.06	4190
19	651566	3408521	0.026	1.03	4250
20	650961	3408808	0.024	0.58	4135
21	650269	3409260	0.030	0.47	4076
22	649773	3409601	0.029	1.06	4122
23	649224	3409558	0.033	0.60	4190
24	648657	3409673	0.031	1.02	4116
25	647783	3409460	0.024	1.09	4297
26	646142	3409343	0.023	0.64	4396
27	640266	3411446	0.021	1.25	3280
28	640674	3412158	0.020	1.11	4046
29	641115	3412073	0.020	1.40	4041
30	642122	3411965	0.023	1.31	4041
31	641479	3411141	0.026	0.75	3355

Table 5. Discharge and TDS at the inlets and outlet of marsh (measured during the period from 3 May 2015 to 28 May 2015).

Station	Date	Discharge (m3/sec)	TDS (ppm)
BC3	3/5/2015	1.63	3151
BC4	3/5/2015	1.52	3040
FBC3	3/5/2015	1.81	3048
FBC4	3/5/2015	2.26	2079
FW	3/5/2015	4.01	2454
Um Nakhla	4/5/2015	2.35	4350
Al-Kurmashia	4/5/2015	1.52	3318
Al-Qausy Drain	3/5/2015	3.32	8791
Al-Hamedy	4/5/2015	2.16	3236
Al-Khamissiya	4/5/2015	29.42	6635
Outlet pipes	3/5/2015	47.26 (water level=1.56 m a.s.l.)	9000

BC3	27/5/2015	1.60	3240
BC4	27/5/2015	1.54	3122
FBC3	27/5/2015	1.78	3036
FBC4	27/5/2015	2.22	2127
FW	27/5/2015	3.26	3025
Um Nakhla	28/5/2015	2.83	3850
Al-Kurmashia	28/5/2015	1.75	2800
Al-Qausy Drain	27/5/2015	3.60	8695
Al-Hamedy	28/5/2015	3.04	3314
Al-Khamissiya	28/5/2015	11.8	6817
Outlet pipes	27/5/2015	32.40 (water level=1.48 m a.s.l.)	8904

2.3. Hydrodynamic and Contaminant Transport Simulation Models

Generally, many software programs can be used to simulate the hydrodynamic and contaminant transport within water bodies. In recent years, the Surface Water Modeling System (SMS) software (Aquavio LLC Provo-Utah-United States, <http://www.aquaveo.com/technical-support/>) has become commonly used. The SMS software includes a variety of models that compute flow velocities and water depths for surface water bodies for both unsteady-state and steady-state conditions, such as RMA2. Additionally, it supports computation of water quality distribution patterns for surface water by using the RMA4 model. RMA2 solves the momentum conservation equations, eqs. (1) and (2), and the continuity equation, eq. (3), which represent the water flow equations in two directions [38].

$$h \frac{\partial u}{\partial t} + hu \frac{\partial u}{\partial x} + hv \frac{\partial u}{\partial y} - \frac{h}{\rho} \left[E_{xx} \frac{\partial^2 u}{\partial x^2} + E_{xy} \frac{\partial^2 u}{\partial y^2} \right] + gh \left[\frac{\partial a}{\partial x} + \frac{\partial h}{\partial x} \right] + \frac{g u n^2}{(1.486 h^{1/6})^2} (u^2 + v^2)^{1/2} - \zeta V_a^2 \cos \psi - 2h v \omega \sin \Phi = 0 \quad (1)$$

$$h \frac{\partial v}{\partial t} + hu \frac{\partial v}{\partial x} + hv \frac{\partial v}{\partial y} - \frac{h}{\rho} \left[E_{yx} \frac{\partial^2 v}{\partial x^2} + E_{yy} \frac{\partial^2 v}{\partial y^2} \right] + gh \left[\frac{\partial a}{\partial y} + \frac{\partial h}{\partial y} \right] + \frac{g v n^2}{(1.486 h^{1/6})^2} (u^2 + v^2)^{1/2} - \zeta V_a^2 \sin \psi - 2h u \omega \sin \Phi = 0 \quad (2)$$

$$\frac{\partial h}{\partial t} + h \left(\frac{\partial u}{\partial x} + \frac{\partial v}{\partial y} \right) + u \frac{\partial h}{\partial x} + v \frac{\partial h}{\partial y} = 0 \quad (3)$$

where h is the water depth; u and v are the velocities in Cartesian coordinates; x and y are the Cartesian coordinates; t is the time; ρ is the density of the fluid; E_{xx} is the eddy viscosity coefficient on the x -axis surface; E_{yy} is the eddy viscosity coefficient on the y -axis surface; E_{xy} and E_{yx} are the shear directions on each surface; ξ is the empirical wind shear confine; g is the acceleration due to gravity; n is the Manning's roughness n -value; a is the elevation of the bottom; V_a is the wind speed; ψ is the wind direction; ω is the rate of earth angular rotation; ϕ is the local latitude; c is the concentration of pollutant for a given constituent; D_x and D_y are the turbulent mixing dispersion coefficients; K_c is the first order decay of the pollutant; $R(c)$ is the rainfall/evaporation rate; and σ is the source/sink of the constituent.

Limitations of the RMA2 model are as follows: the pressure is hydrostatic, mean acceleration has a vertical direction, vibration and vortices are neglected, and water density is constant, and it uses a horizontal two-dimensional plane. Additionally, problems in calculating the free surface for subcritical flow were not carried out, and areas of vertically stratified flow are beyond this program's capabilities [39].

For contaminant transport simulations, the transport of a constituent is calculated based on the depth-averaged transport and mixing process equation, which is given by eq. (4). The RMA4 model solves this equation to simulate contaminant transport in a free surface water body [38].

$$h \left[\frac{\partial c}{\partial t} + u \frac{\partial c}{\partial x} + v \frac{\partial c}{\partial y} - \frac{\partial}{\partial x} D_x \frac{\partial c}{\partial x} - \frac{\partial}{\partial y} D_y \frac{\partial c}{\partial y} - \sigma + k_c + \frac{R(c)}{h} \right] = 0 \quad (4)$$

The use of this model is limited to average depth (two-dimensional) situations, and the accuracy of the transport model is dependent on the accuracy of the hydrodynamic model of the water body [39].

2.3.1. Hydrodynamic Model (RMA2)

Although the real state of flow within the marsh is unsteady and the flow must be simulated using an unsteady model, the flow within the marsh was assumed to be steady. The significance and consequence of this assumption can be ignored because the change in inflow and outflow water levels and discharges (upstream and downstream boundary conditions) of the marsh is very slow. Additionally, the velocity of flow within the marsh is low. However, a two-dimensional hydrodynamic model (RMA2) was conducted to simulate the flow within the marsh. This model was performed according to the following four steps:

First, the geometric data were prepared. The DEM of the study area, which is shown in Figure 3, was the input file of the topographical data, whereas Figure 2, [34], was used to delineate the boundary of the marsh to create the shapefile of the marsh boundary.

Second, finite element mesh was generated. Based on the created shapefile of the marsh boundary, the conceptual model was converted to create a finite element mesh. The generated mesh of the marsh has 29384 nodes, which formed 14407 triangular elements. However, the mesh was edited to enhance the numerical stability and efficiency.

Third, the boundary conditions were specified. According to the results of the analyses of the present and potential cases of the marsh flow data, which are the 30 cases listed in Table 2, the inflow discharges at the inlet and the corresponding water levels at the outlets were used as the upstream and downstream boundary conditions, respectively. The calibration and verification processes were performed by using field observation measurements from 3 May 2015 to 4 May 2015 and 27 May 2015 to 28 May 2015, respectively (Table 5).

Finally, the material properties were specified. The material properties are essential input data in the RMA2 model. Hence, each cell in the finite element mesh must assigned a value for eddy viscosity [38]. The friction coefficient of the material of each cell was represented by the roughness-depth relationship presented by [35], as shown in Figure 4. However, the validity and reliability of using this relationship within this part of the marsh was checked through the calibration process.

2.3.2. Contaminant Transport Models (RMA4)

A two-dimensional contaminant transport simulation model was prepared using the RMA4 model to estimate the patterns of TDS distribution within the marsh. The implementation of this model was based on the results of the RMA2 model. In accordance with the modeled potential cases of marsh boundary conditions using the RMA2 model, which are the 30 cases listed in Table 2, the corresponding TDS concentrations at the inlets for the potential cases of marsh boundary conditions for the RMA4 model (Table 3) were used as upstream boundary conditions for the RMA4 model. However, the discharges and TDSs at the inlets and the water level at the outlet of the marsh measured on 27 May 2015 and 28 May 2015 (Table 5) were used to perform the verification process of the RMA4 model.

2.4. Spatial and Temporal Analysis

Based on the results of applying RMA4 for all the considered potential cases, which are the 30 cases listed in Table 2, the TDS transport within the marsh was investigated to specify the time interval between the occurrence of successive detectable changes in the TDS concentrations (within ALC of $\pm 5\%$) in each MS. Consequently, the minimum interval of change occurrence for each MS can be specified. For this purpose, the spatial and temporal analysis tools of GIS, which provide flexibility in handling the large amount of spatial and temporal data, were used. A spatiotemporal analysis approach that uses time as the organizational basis [40, 41] was used to analyze the patterns of TDS distribution. Accordingly, considering that the locations of the MSs are the optimal locations, the best time schedule of SF for all the considered MSs can be implemented. This time schedule ensures the detection of all the effective changes in water quality and confirms that no pollution surge passes any MS without detection. In addition, to evaluate the effect of changing the ALC, the results of the RMA4 model (TDS distribution patterns) were reanalyzed using the spatiotemporal analysis approach and increasing ALC to $\pm 10\%$ and $\pm 15\%$ for each case of boundary conditions.

3. Results and Analysis

3.1. Verification of the RMA2 and RMA4 Models

The verification process was performed to evaluate the certainty of using the roughness-depth relationship of the marsh bed given by Manning's roughness coefficient (Figure 3), which was recommended by [35] and the accuracy of the implemented RMA2 model of the marsh. Two sets of measured data were used to perform the verification process (Table 5). The first set is the measured data on 3 May 2015 and 4 May 2015, whereas the second set is the measured data on 27 May 2015 and 28 May 2015. These sets were applied as boundary conditions to implement two RMA2 models for the marsh; the two models that correspond to the first and second set of measured data were named RMA2-1 and RMA2-2, respectively. The friction coefficient of the marsh bed materials was represented by the roughness-depth relationship. Then, the measured water depths at 31 points within the marsh on 27 May 2015 and 28 May 2015 (Table 4) were compared with those estimated by applying the RMA2-1 model at the same points. Additionally, at the same points, the measured flow velocity were compared with those estimated by applying the RMA2-2 model. These comparisons showed that the root mean square error (RMSE) of the water depth was 0.19 m, whereas the RMSE of the flow velocity was 0.005 m/sec. However, considering the intricacy of the geometry, feeding and outflow system, and the land use and land cover aspects of the marsh, this level of certainty in using the roughness-depth relationship, which was recommended by [35], ensures that the accuracy of the RMA2 model results can be accepted.

Based on the results of the verified RMA2 models, an RMA4 model was implemented to obtain the patterns of TDS distribution. The measured TDS data on 27 May 2015 and 28 May 2015 at the inlets of the marsh (Table 5), were used as boundary conditions for the RMA4 model. Comparison between the measured and estimated TDS values at 31 points showed that the RMSE was 492 ppm. Hence, the implemented RMA4 model is sufficient to simulate the distribution of TDS within the marsh.

3.2. Application of the RMA2 and RMA4 Models

The RMA2 and RMA4 models were consecutively applied for the potential cases of marsh boundary conditions, which are the 30 cases listed in Table 2. Samples of the results of the RMA2 and RMA4 models are shown in Figures 6 to 8. These figures show the patterns of flow velocity and TDS distribution within the marsh for cases 1, 15 and 30, which can be considered as the cases of maximum, average and minimum inflow, respectively.

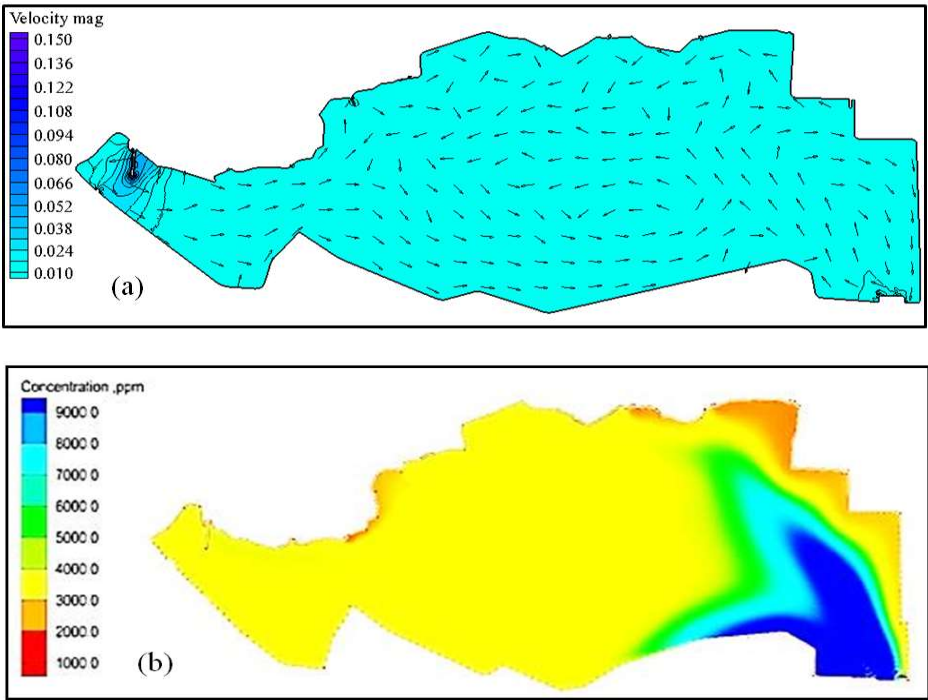


Figure 6. Distribution patterns of the flow velocity and TDS for the maximum inflow (Case 1). (a) Velocity pattern. (b) TDS pattern.

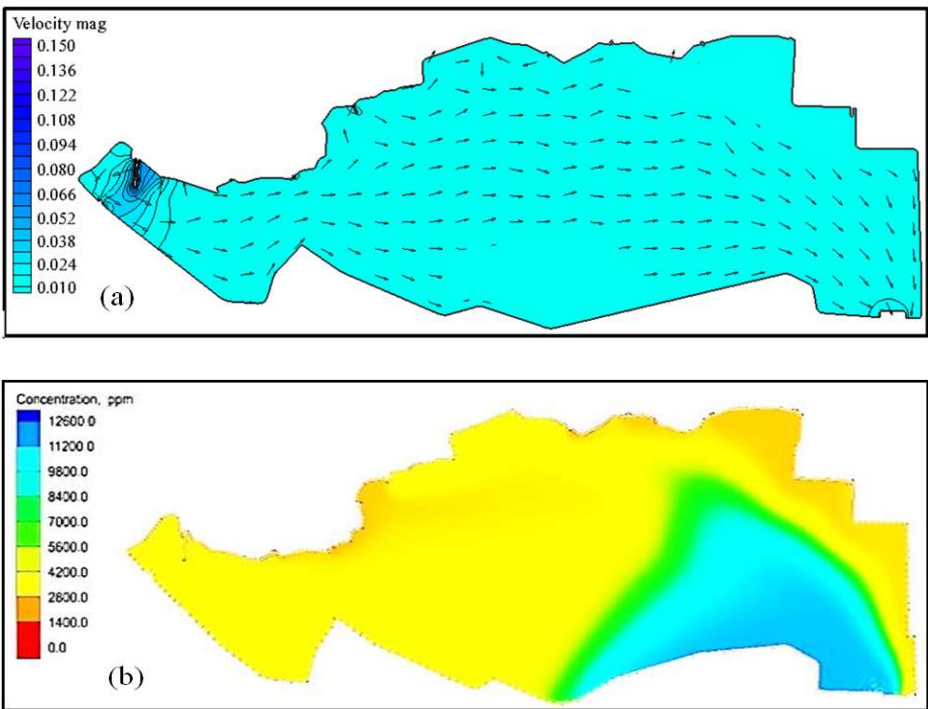


Figure 7. Distribution patterns of the flow velocity and TDS for the average inflow (Case 15). (a) Velocity pattern. (b) TDS pattern.

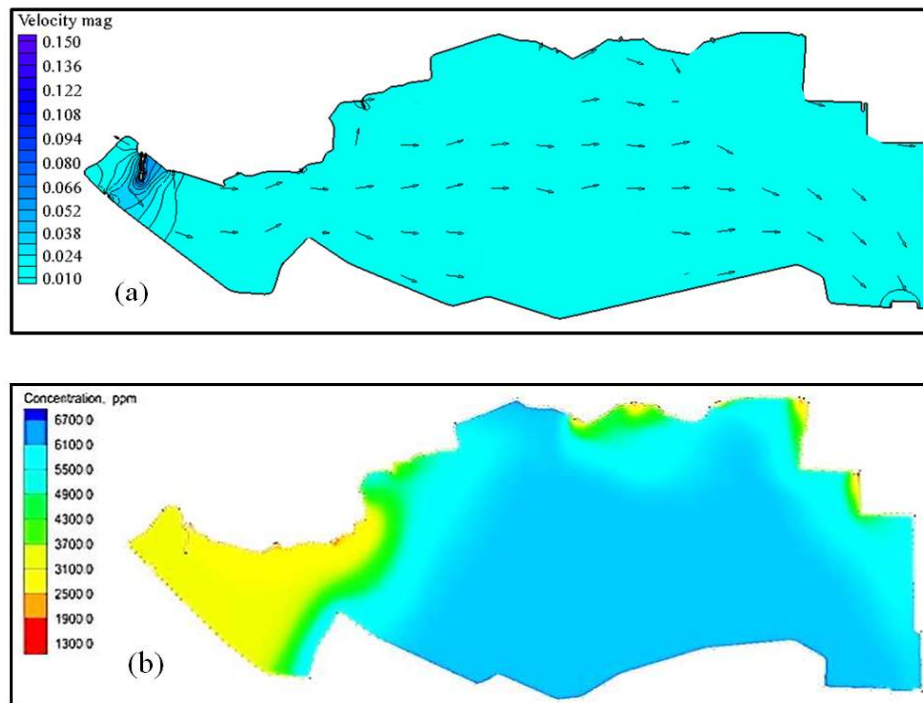


Figure 8. Distribution patterns of the flow velocity and TDS for the minimum inflow (Case 30). (a) Velocity pattern. (b) TDS pattern.

The results of the RMA4 model of the 30 considered cases were analyzed using the spatial and temporal analysis tools of GIS. The approach of time-based representations for spatiotemporal data [41] was applied to obtain the time interval of occurrence of a considerable level of change in the concentration of TDS (ALC of $\pm 5\%$) at all the studied MSs (46 MSs). Accordingly, the minimum, average and maximum SFs (time intervals) were determined for all the considered 46 MSs (Figure 9). Hence, the SFs of other cases ranged between the SFs of these cases. However, the results of the spatiotemporal analyses show that the minimum SF interval is 11 *days*. This SF was estimated at 26% of the MSs, which are MS numbers 15, 16, 17, 19, 20, 21, 22, 23, 29, 30, 31 and 36. These MSs are located within the central and outlet zone of the marsh, except for MS number 36, which is located in the narrow part of the western zone of the marsh. Furthermore, 52% of the MSs have an SF equal to or greater than 14 *days*. Additionally, a maximum interval of SF of 32 *days* was estimated at 17% of the MSs, which are MS numbers 18, 19, 20, 21, 22, 23, 27 and 28. The change in SF from minimum to maximum time interval is based on the considered case of boundary conditions.

To evaluate the effect of changing the ALC, the results of the RMA4 model (TDS distribution patterns) were reanalyzed using the spatiotemporal analysis approach and increasing ALC to $\pm 10\%$ and $\pm 15\%$. The results of the spatiotemporal analyses show that increasing the ALC to $\pm 10\%$ and $\pm 15\%$ increases the minimum SF for some MSs by approximately 18% and 21%, respectively, as shown in Figures 10 and 11. With an ALC of $\pm 10\%$, 26% of the MSs have a minimum interval of SF of 13 *days*, whereas the maximum interval of SF was 35 *days*, which is estimated at 15% of the MSs. However, with an ALC of $\pm 15\%$, 15% of the MSs have a minimum SF interval of 13 *days*, whereas the maximum interval of SF was 36 *days*, which is estimated at 9% of the MSs.

Comparatively, a sampling schedule (Figure 12) was implemented based on the criteria of the sampling frequency for GEMS/WATER stations shown in Table 1 [23]. This time schedule specifies the number of samples and SF for the marsh. According to this schedule, one sample should be taken seasonally from each location within the marsh, whereas for the feeders and outlet, this number depends on the discharge, and each should be taken at least two times per month.

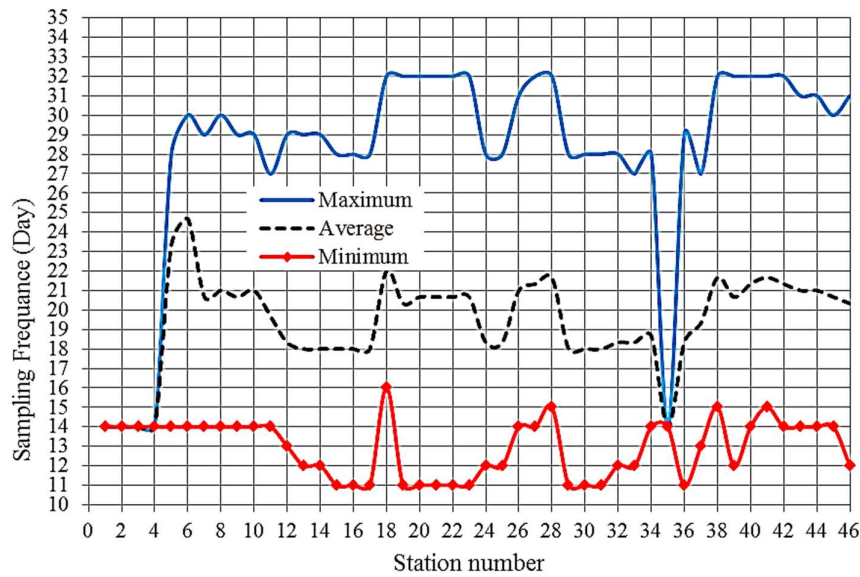


Figure 9. Minimum, average and maximum interval of SF of the 46 MSs (ALC of $\pm 5\%$).

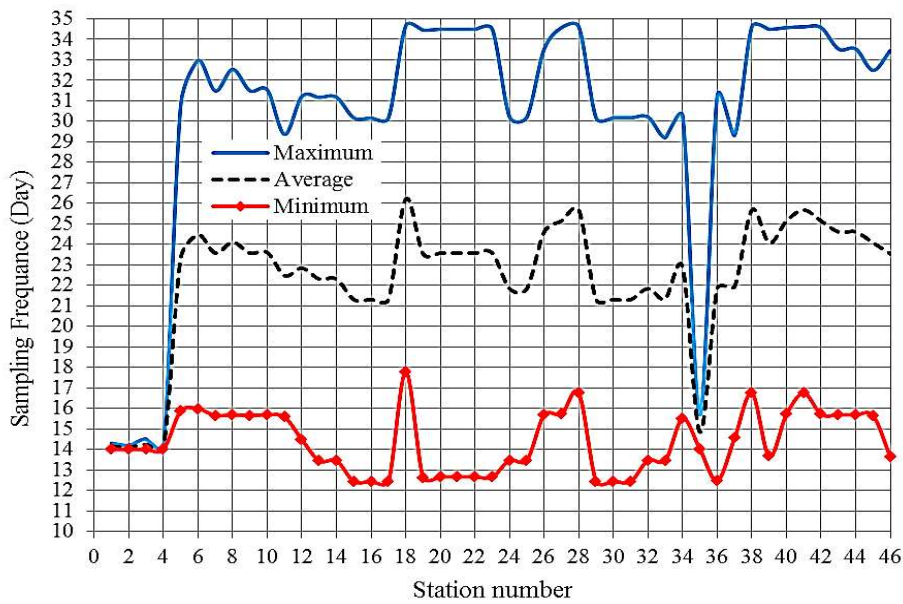


Figure 10. Minimum, average and maximum interval of SF of the 46 MSs (ALC of $\pm 10\%$).

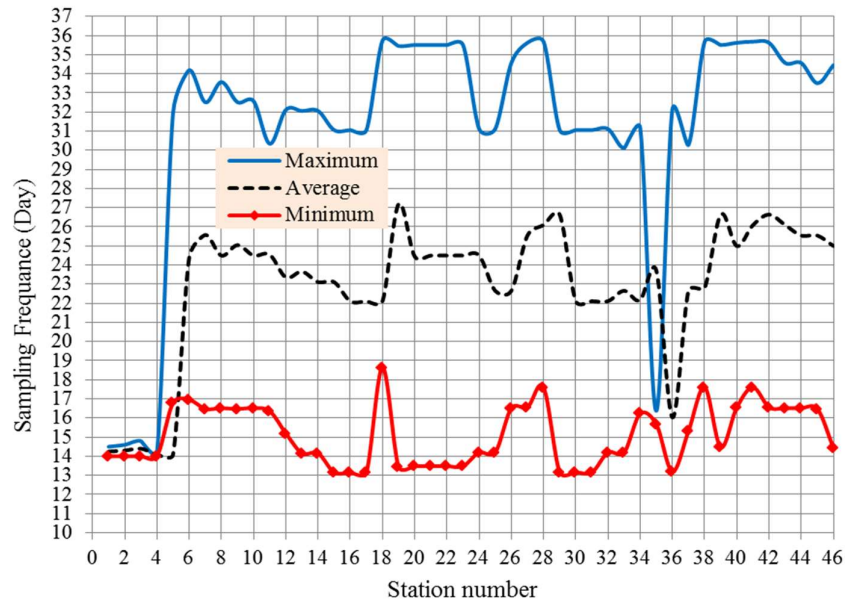


Figure 11. Minimum, average and maximum interval of SF of the 46 MSs (ALC of $\pm 15\%$).

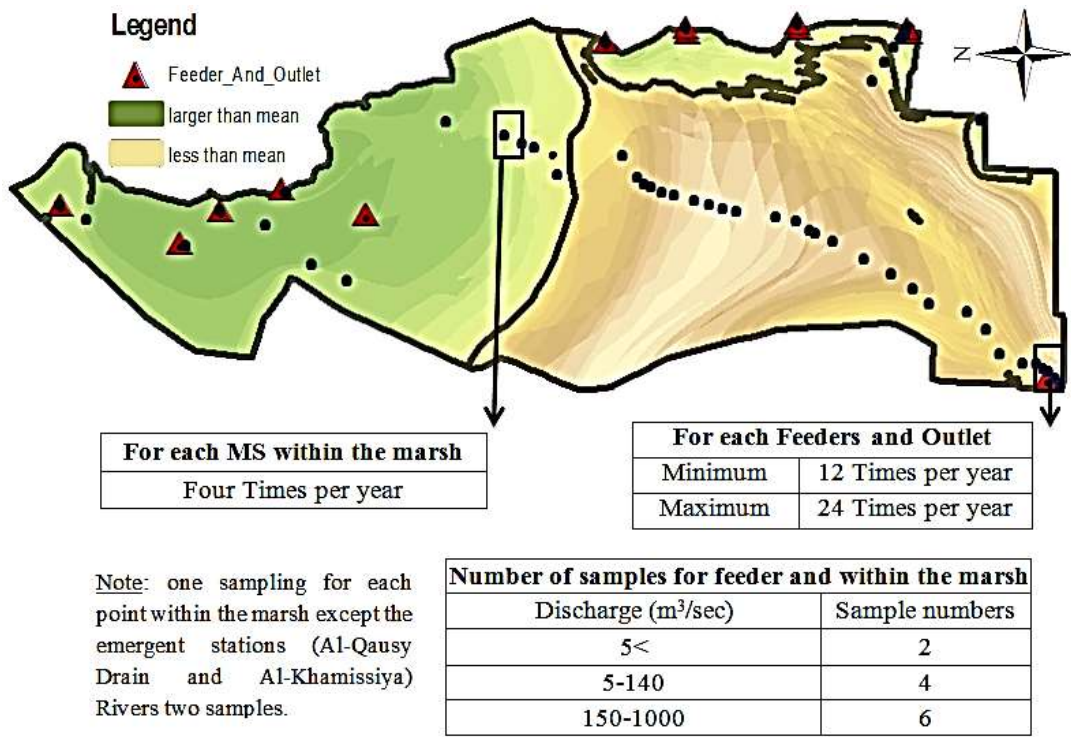


Figure 12. Sampling schedule using [23].

Application of these general guidelines and criteria present a very permissive schedule of SF, which is four times per year. The proposed methodology specifies a minimum and maximum SF interval for each MS that ranged between 33 and 12 times per year (11 and 32 days), respectively. This difference is because applying the general guidelines and criteria does not consider the difference in the sensitivity of pollution detection of the MSs, status of changes of the boundary conditions, complexity of the feeding and drainage system, or analysis of the contaminant distribution patterns. Hence, this traditional design approach does not ensure sufficient detection of all potential pollution waves.

However, the proposed methodology includes all the potential values and cases of boundary conditions, which increases the certainty of monitoring the system and the efficiency of the SF schedule. The possibility of occurrence of a case outside of the extreme limits of the boundary conditions is very unlikely. Even if such a case occurs, there is still a high probability that the SF schedule ensures the detection of the changes in pollution level and monitors the flow of pollution surges. This is because the proposed methodology depends on the analysis of the contaminant distribution patterns and the transport velocity of the pollution surges through highly sensitive MSs for the changes in boundary conditions. Additionally, the pollution levels within the water body are highly expected to be within the recorded pollution levels. Even if there is a difference, the transport velocity of the pollution surge between the MSs and the duration of change in pollution level at each MS will not differ much from the specified range using this proposed methodology. Moreover, the hydrodynamic (Advection) flow has a greater effect on contaminant transport than that of the diffusion. Therefore, the change in contaminant concentration and location of pollution source within the considered body of water and range of hydraulic changes would not have a large effect on the velocity of the pollution surges, especially considering that the MSs are allocated at the most sensitive locations.

4. Conclusions

Exacerbation of the water scarcity problem in conjunction with the increase in water pollution sources necessitates the development of methods and techniques for water quality monitoring. However, most of the applied design methods are statistical methods and general criteria. These methods are based on a measured dataset collected from nonoptimal preallocated monitoring stations (MS). Therefore, insufficient monitoring is obtained because some effective events or values may not be detected. In this paper, a novel deterministic methodology for estimating the optimal SF for WQMSs has been developed. To this end, contaminant transport simulation models and the GIS tools of spatiotemporal analysis were employed to ensure detection of a specific level of change in a contaminant concentration considering all the potential changes in the boundary conditions of a water body. The simulation models and GIS tools were applied to the potential cases of the boundary conditions of Al-Hammar Marsh to determine the minimum SF of the previously allocated 46 MSs with ALC values of $\pm 5\%$, $\pm 10\%$ and $\pm 15\%$. Subsequently, the obtained SF schedule using the proposed methodology was compared with those obtained by applying the criteria of GEMS/WATER stations [23]. From the analysis of the results, it can be concluded that the changes in contaminant transport patterns within a water body essentially depend on the cases and values of the boundary conditions. Therefore, the accuracy of monitoring stations at the feeders and outlets of a water body plays a vital role in the accuracy of the obtained SF using any method of determining the SF. Additionally, the geometrical features of a water body or its zones highly affect the velocity and direction of the contaminant distribution within the zones of the water body between the monitoring stations. Consequently, the response of the change in contaminant distribution to the change in boundary conditions differs among the zones of the water body, which affects the determined SF. The SF is highly affected by the values of ALC. However, in the considered study area (the western part of the Al-Hammar Marsh), increasing the ALC from $\pm 5\%$ to $\pm 10\%$ and $\pm 15\%$ increases the minimum SF for some MSs by approximately 18% and 21%, respectively. Hence, the proposed methodology can be used to compute the SF needed to detect a contaminant between MSs within a specific level of ALC and vice versa. Utilizing the general criteria and guidelines may give a very permissive schedule of SF. However, in the western part of the Al-Hammar Marsh, applying the general guidelines and criteria gives an SF of four times per year. In contrast, the proposed methodology specifies a maximum and minimum interval of SF for each MS that ranged between 33 and 12 times per year, respectively. The proposed methodology is based on considering all the potential types and values of boundary conditions of the water body. This increases the certainty of the obtained SF and the efficiency of the monitoring system beyond those obtained using other methods. Moreover, the proposed methodology can be applied to all types of surface water resources and can consider any number of MSs with any accuracy level of detectable change. In

addition, the proposed methodology provides a detailed database for the distribution patterns of the considered contaminant with the corresponding case and values of boundary conditions.

Funding: This research received no external funding.

Acknowledgments: I would like to particularly thank the University of Technology, Baghdad, Iraq, for their valuable scientific assistance and support. Many institutions contributed to this research in various ways. I would like to thank the Iraqi Ministry of Water Resources for providing the required data and technical assistance. It is inevitable that many people have contributed to this work, and I would like to acknowledge the support and assistance I have received from several friends and colleagues.

Conflicts of Interest: The author declare no conflict of interest

References

1. Bu, H.; Tan, X.; Li, S.; Zhang, Q. Temporal and spatial variations of water quality in the Jinshui River of the South Qinling. *Mts Ecotoxicol Environ Saf*, 2010, Vol. 73, no. 5, pp. 907-913. <http://dx.doi.org/10.1016/j.ecoenv.2009.11.007>
2. Behmel, S.; Damour, M.; Ludwig R.; Rodriguez, M.J. Water quality monitoring strategies—A review and future perspectives. *Sci. Total Environ.* 2016, Vol. 571, 1312–1329. <https://doi.org/10.1016/j.scitotenv.2016.06.235>
3. Thomas, G. S.; Adrian, D. D. Sampling frequency for river quality monitoring. *Water resources research*. 1978, Volume14, Issue4, Pages 569-576
4. Loftis, J.C.; Ward, R.C. Water quality monitoring - Some practical sampling frequency considerations. *Environmental Management*, 1980, 4, 6, (521-526). <https://doi.org/10.1007/BF01876889>
5. Robert, H.H.; Michael, J.B. Sampling frequency for water quality monitoring. Advanced Monitoring Systems Division, Environmental Monitoring Systems Laboratory, Las Vegas, Nevada 89114, 1981.
6. Skalski, J.R.; Mackenzie, D.H. A design for aquatic monitoring programs. *J. Environ. Manage*, 1982, 14, 237–251.
7. Don, C.; Peter, N. N.; Dean, H. U. Sampling frequency for water quality monitoring: Measures of effectiveness. *Water resources research*, 1983, Volume19, Issue5, Pages 1107-1110. <https://doi.org/10.1029/WR019i005p01107>.
8. Groot, S.; Schilperoort, T. Optimization of water quality monitoring networks. *Wat. Sci. tech.*, 1984, 16(5-7), 275-287.
9. Steven, P.M.; Dennis, P.L. Optimal design of biological sampling programs using the analysis of variance. *Estuarine, Coastal and Shelf Science*, 1986, 22, 5, (637-656). [https://doi.org/10.1016/0272-7714\(86\)90018-1](https://doi.org/10.1016/0272-7714(86)90018-1)
10. Smith, D.G.; McBride, G.B. New Zealand's National Water Quality Monitoring Network – Design and First Year's Operation. *Water Resources Bulletin*, 1990, 26(5):767-775.
11. Loftis, J.C.; McBride, G.B.; Ellis, J.C. Considerations of scale in water quality monitoring and data analysis. *Water Resources Bulletin*, 1991, 27(2): 255- 264. <https://doi.org/10.1111/j.1752-1688.1991.tb03130.x>
12. Esterby, S.R.; El-Shaarawi, A. H.; Block, H.O. Detection of water quality changes along a river system. *Environ. Monit. Assess.* 1992, 23, 219–242. <https://doi.org/10.1007/BF00406963>
13. Yangxiao, Z. Sampling frequency for monitoring the actual state of groundwater systems. *Journal of Hydrology*, 1996, 180, 1-4, (301-318). [https://doi.org/10.1016/0022-1694\(95\)02892-7](https://doi.org/10.1016/0022-1694(95)02892-7)
14. Dixon, W.; Chiswell, B. Review of aquatic monitoring program design. *Water Res.* 1996, 30, 1935–1948. [https://doi.org/10.1016/0043-1354\(96\)00087-5](https://doi.org/10.1016/0043-1354(96)00087-5)
15. Charles, G. H. Relationships between total phosphorus concentrations, sampling frequency, and wind velocity in a shallow, Polymictic Lake, *Lake and Reservoir Management*, 1999, 10.1080/07438149909353950, 15, 1, (39-46).
16. Ning, S.K.; Chang, N.B. Multi-objective, decision-based assessment of a water quality monitoring network in a river system. *J. Environ. Manage*, 2002, 4, 121–126. <https://doi.org/10.1039/B107041J>
17. Su-Young, P.; Jung, H. C.; Sookyun, W.; Seok, S. P. Design of a water quality monitoring network in a large river system using the genetic algorithm, *Ecological Modelling*, 2006, 199, 3, (289-297), 10.1016/j.ecolmodel.2006.06.002.

18. Loftis, J.C.; Ward, R.C. Sampling frequency selection for regulatory water quality monitoring, *Journal of the American Water Resources Association*, 2007, 16, 3, (501-507). <https://doi.org/10.1111/j.1752-1688.1980.tb03904.x>
19. Harmancioglu, N.B.; Alpaslan, N. Water quality monitoring network design: a problem of multiobjective decision making. *Water Resour Bull*, 1992, 28(1): 179–192. <https://doi.org/10.1111/j.1752-1688.1992.tb03163.x>
20. Hudak, P.F.; Loaiciga, H.A.; Marino, M.A. Regional-scale ground water quality monitoring via integer programming. *J. Hydrol.* 1995, 164, 153–170. [https://doi.org/10.1016/0022-1694\(94\)02559-T](https://doi.org/10.1016/0022-1694(94)02559-T)
21. Cieniawski, S. E.; Eheart, J. W.; Ranjithan, S. Using genetic algorithms to solve a multiobjective groundwater monitoring problem. *Water Resour. Res.* 1995, 31, 399–410. <https://doi.org/10.1029/94WR02039>
22. Strobl, R.O.; Robillard, P.D. Network design for water quality monitoring of surface freshwaters: a review. *Journal of Environmental Management*, 2008, 87, 639–648. <https://doi.org/10.1016/j.jenvman.2007.03.001>
23. UNEP/WHO. Water Quality Monitoring - A Practical Guide to the Design and Implementation of Freshwater Quality Studies and Monitoring Programmes Edited by Jamie Bartram and Richard Ballance Published on behalf of United Nations Environment Programme and the World Health Organization © 1996 UNEP/WHO ISBN 0 419 22320 7 (Hbk) 0 419 21730 4 (Pbk).
24. Timmerman, J.G.; Adriaanse, M.; Breukel, R.M.A.; Van Oirschot, M.C.M.; Ottens, J.J. Guidelines for water quality monitoring and assessment of transboundary rivers. *Euro. Water Pollut. Control*, 1997, 7, 21–30. journal ISSN :0925-5060
25. Dixon, W.; Smyth, G.K.; Chiswell, B. Optimized selection of river sampling sites. *Water Res.* 1999, 33, 971–978. [https://doi.org/10.1016/S0043-1354\(98\)00289-9](https://doi.org/10.1016/S0043-1354(98)00289-9)
26. Khalil, B.; Ouarda, T.B. Statistical approaches used to assess and redesign surface water-quality-monitoring networks, *Journal of Environmental Monitoring*, 2009, 11, (1915). <https://doi.org/10.1039/B909521G>
27. World Meteorological Organization. Planning of Water Quality Monitoring System. Technical Report, 2013, Series No. 3 World Meteorological Organization, CH-1211 Geneva 2, Switzerland, ISBN 978-92-63-11113-5).
28. Don, C.; Peter, N. N.; Dean H. U. Sampling frequency for water quality monitoring: Measures of effectiveness. *Water resources research*, 1983, Volume19, Issue5, Pages 1107-1110. <https://doi.org/10.1029/WR019i005p01107>
29. Kaya, I.; Kahraman, C. Multicriteria decision making in energy planning using a modified fuzzy TOPSIS methodology. *Expert Syst Appl*, 2011, 38(6):6577–6585. <https://doi.org/10.1016/j.eswa.2010.11.081>
30. Huu, T. D.; Shang-Lien, L.; Lan Anh, P. T. Calculating of river water quality sampling frequency by the analytic hierarchy process (AHP). *Environ Monit Assess*, 2013, 185:909–916, <https://doi.org/10.1007/s10661-012-2600-6>.
31. Holnicki P, Nahorski Z, Żochowski A. Modelling of Environment Processes. Warszawa: Wydawnictwo Wyższej Szkoły Informatyki Stosowanej i Zarządzania; 2000.
32. Balcerzak, W. Application of selected mathematical models to evaluate changes in water quality. In: *International Conference on Water Supply, Water Quality and Protection*. Kraków, 2000.
33. WMO (World Metrological Organization). Guide to hydrological practice, 2008, Vol. I, No. 168. Sixth Edition. World Metrological Organization, Geneva, Switzerland.
34. Al-Khafaji, M.S.; Abdulraheem, Z.A. A deterministic algorithm for determination of optimal water quality monitoring stations. *Water Resour Manage*, 2017, 31: 3575. <https://doi.org/10.1007/s11269-017-1686-6>.
35. Alhamdani, J.S. Location of outlet and operation of the west part of Al-Hammar Marsh. Ph. D. Thesis, University of Baghdad, Iraq, 2014.
36. Iraqi Ministry of Environment, New Eden master plan for the integrated water resources management in the Marshland area, Marshlands, Book 4, Iraqi Ministries of Environment, Water Resources Municipalities and Public Works with cooperation of the Italian Ministry for the Environment and Territory and Free Iraq Foundation, 130, 2006.
37. Donnell, B.P.; Letter, J.V.; McAnally, W.H.; others. User Guide to WES-RMA2 Version 4.5. Waterways Experiment Station, Costal and Hydraulics Laboratory, 2004a, California, Davis.
38. Donnell, B.P.; Letter, J.V.; McAnally, W.H.; others. User Guide to WES-RMA4 Version 4.5. Waterways Experiment Station, Costal and Hydraulics Laboratory, 2004b, California, Davis.

39. Peuquet, D. J.; Duan, N. An event-based spatio-temporal data model (ESTDM) for temporal analysis of geographic data. *International Journal of Geographical Information Systems*, 1995, 9: 2–24. <https://doi.org/10.1080/02693799508902022>
40. Peuquet, D. J.; Wentz, E. An approach for time-based analysis of spatio-temporal data. Sixth International Symposium on Spatial Data Handling, Edinburgh, Scotland. International Geographical Union, 1994, 489–504.